

Evolutions from extremality

Ivan Booth*

*Department of Mathematics and Statistics
Memorial University of Newfoundland
St. John's, Newfoundland and Labrador, A1C 5S7, Canada*

(Dated: March 18, 2016)

We examine the evolution of extremal spherically symmetric black holes, developing both general theory as well as the specific cases of (charged) null dust and massless scalar field spacetimes. As matter accretes onto extremal marginally trapped tubes, they generically evolve to become non-extremal with the initial extremal horizon bifurcating into inner and outer non-extremal horizons. At the start of this process arbitrarily slow matter accretion can cause a geometrically invariant measure of horizon growth to jump from zero to infinity. We also consider dynamical horizons that are extremal throughout their evolution and see that such spacetimes contain two extremal black hole horizons: an inner isolated one and an outer dynamical one. We compare these extremal dynamical horizons with the dynamical extreme event horizon spacetimes of Murata, Reall and Tanahashi.

I. INTRODUCTION

Extremality plays an important role in the mathematics and physics of black holes. Thermodynamically, extremal black holes are zero temperature states and subject to the third law of black hole mechanics: physical processes cannot turn a non-extremal hole into an extremal one[1]. Supersymmetric black holes are necessarily extremal and this made the first string theory calculations of black hole entropy possible[2]. Physically, for any given horizon area, black holes have a maximum charge and rotation and those bounds are saturated by extremal holes[3–6]. Mathematically their horizon geometry is tightly constrained in any dimension and indeed in four-dimensions the intrinsic geometry of any extremal horizon in Einstein-Maxwell theory is isometric to a member of the Kerr-Newman family[7]. Through the near horizon formalism, the tight constraints have also enabled great progress in the classification of (time-independent) extremal black hole horizons in five and higher dimensions [8].

Most of the work mentioned in the preceding paragraph has focussed on stationary extremal black holes. However it has recently been shown that these very important solutions are unstable and so not expected to remain stationary under generic conditions. The initial proof of the instability of extremal Reissner-Nordström black holes [9, 10] was quickly extended to Kerr-Newman black holes [11–13]. Subsequent work has included numerical probes of that instability [14, 15].

Given these instabilities it is of interest to understand the evolution of initially extremal black holes and in this paper we study both exits from extremality and special cases of dynamical extremal horizons. Somewhat surprisingly such evolutions have not received much attention in the literature. As such there are simple yet

still interesting cases that have not been studied and we tackle one of them here. We restrict our attention to spherically symmetric spacetimes and focus our attention mainly on the evolution of the marginally trapped tubes (essentially apparent horizons) though we will also briefly consider event horizons. We primarily use Vaidya Reissner-Nordström (VRN) spacetimes as concrete examples but also briefly consider massless scalar fields.

This paper is organized as follows. Section II develops the general theory of marginally trapped tubes in spherically symmetric backgrounds. It sets up notation and reviews two-surface geometry both in general and as applied to geometric horizons. It then considers the kinematics and dynamics of those horizons. Section III considers the special case of null dust accreting onto an existing black hole. It reviews Vaidya Reissner-Nordström and then examines both transitions from extremality and evolutions at extremality. Section IV explores some of the results of Murata, Reall and Tanahashi [15], first considering the interaction of extremal horizons and massless scalar fields and then examining dynamical extremal event horizons. Finally Section V reviews and discusses our results.

II. BACKGROUND AND GENERAL THEORY

In this section we establish the background material that we will need for the calculations: the geometry of two-surfaces, definitions of geometric horizons and the kinematics and dynamics of marginally trapped tubes. Throughout we restrict our attention to spherically symmetric spacetimes and marginally trapped tubes. For more details on the geometry, using the same notation (including more general non-symmetric cases) see [16].

* ibooth@mun.ca

A. Spacetime and two-surface geometry

Let (M, g_{ab}, ∇_a) be a $(3+1)$ -dimensional spherically symmetric spacetime. By the symmetry it may be decomposed into spacelike two-surfaces $S(t, r)$ where t is a time parameter and r is the areal radius of the surface.

There are four null directions from each surface and we assume that we are working in a spacetime in which those directions may be identified as future/past and inwards/outwards. The spherically symmetric vectors ℓ and n respectively point in the future outward and future inward directions and are cross-normalized so that $\ell \cdot n = -1$. This leaves one degree of rescaling freedom $\ell \rightarrow e^f \ell$ and $n \rightarrow e^{-f} n$ in the null vectors. We assume that the scaling is also spherically symmetric so that the allowed freedom is given by $f = f(t, r)$.

The induced metric on the two-surfaces is

$$\tilde{q}_{AB} dx^A dx^B = r^2 d\Omega^2 \quad (1)$$

where $d\Omega^2$ is the usual metric on the unit two-sphere while their outward and inward expansions are respectively:

$$\theta_{(\ell)} = \frac{1}{\sqrt{\tilde{q}}} \mathcal{L}_\ell \sqrt{\tilde{q}} = 2\mathcal{L}_\ell \ln(r) \quad \text{and} \quad (2)$$

$$\theta_{(n)} = \frac{1}{\sqrt{\tilde{q}}} \mathcal{L}_n \sqrt{\tilde{q}} = 2\mathcal{L}_n \ln(r), \quad (3)$$

where \mathcal{L}_ℓ indicates a Lie derivative and $\sqrt{\tilde{q}} = r^2 \sin \theta$ is the area element on the $S(t, r)$. These expansions are used to classify surfaces. In particular we will be interested in *untrapped* surfaces ($\theta_{(\ell)} > 0, \theta_{(n)} < 0$), *trapped* surfaces ($\theta_{(\ell)} < 0, \theta_{(n)} < 0$), *marginally outer trapped* surfaces (MOTS) ($\theta_{(\ell)} = 0$) and *marginally trapped* surfaces (MTS) ($\theta_{(\ell)} = 0, \theta_{(n)} < 0$).

In later sections we will need to know the rates of change of these expansions. These are:

$$\mathcal{L}_\ell \theta_{(\ell)} - \kappa_\ell \theta_{(\ell)} = -G_{ab} \ell^a \ell^b - \frac{1}{2} \theta_{(\ell)}^2 \quad (4)$$

$$\mathcal{L}_n \theta_{(\ell)} + \kappa_n \theta_{(\ell)} = -\tilde{K} + G_{ab} \ell^a n^b - \theta_{(\ell)} \theta_{(n)} \quad (5)$$

$$\mathcal{L}_\ell \theta_{(n)} + \kappa_\ell \theta_{(n)} = -\tilde{K} + G_{ab} \ell^a n^b - \theta_{(\ell)} \theta_{(n)} \quad (6)$$

$$\mathcal{L}_n \theta_{(n)} - \kappa_n \theta_{(n)} = -G_{ab} n^a n^b - \frac{1}{2} \theta_{(n)}^2 \quad (7)$$

where $\tilde{K} = 1/r^2$ is the Gauss curvature of $S(t, r)$ and $\kappa_X = -X^a n_b \nabla_a \ell^b$.

B. MOTTs: definition and classification

There are several closely related geometrical notions of horizon including apparent horizons [17], trapping horizons [18], isolated/dynamical horizons [19], marginally trapped tubes [20] and, most recently, future holographic

screens [21]. A summary of the definitions of these various objects and their complex nomenclature may be found in [22]¹.

In all of these notions horizons are *marginally outer trapped tubes* (MOTTs): three-surfaces H foliated by MOTS. *Isolated horizons* are null and time-independent MOTTs (with tangent ℓ). Essentially they are equilibrium states. In this paper we usually further specialize to *marginally trapped tubes* (MTTs): MOTTs with $\theta_{(n)} < 0$.

A typical black hole also has trapped surfaces inside the horizon and untrapped surfaces outside. That there be outer trapped surfaces “just inside” a spherical MOTS² can be formalized as requiring $\mathcal{L}_n \theta_{(\ell)} < 0$. In Hayward’s classification [18] this is the defining condition for an *outer* trapping horizon. Researchers working with initial data have a slightly stronger condition which they call *strictly stably outermost* (introduced in [23, 24] and much used since). Given a MOTS with outward-pointing spacelike normal \hat{r} in a Cauchy surface Σ this condition requires $\mathcal{L}_{\hat{r}} \theta_{(\ell)} > 0$. Such a vector can always be written as $\hat{r} = A\ell - Bn$ for some positive A and B . Then in spherical symmetry

$$\mathcal{L}_{\hat{r}} \theta_{(\ell)} > 0 \implies \mathcal{L}_n \theta_{(\ell)} < \left(\frac{B}{A}\right) \mathcal{L}_\ell \theta_{(\ell)}. \quad (8)$$

Given the null energy condition $\mathcal{L}_\ell \theta_{(\ell)} < 0$ by (4) and so this implies that a strictly stably outermost MOTS is an outer trapping horizon. For isolated horizons the notions are equivalent.

However, these conditions certainly do not hold for all MOTS. They are characteristic of outer horizons (hence Hayward’s nomenclature) but are violated for inner horizons. For example the inner Cauchy horizon of a non-extremal Reissner-Nordström black hole has $\mathcal{L}_n \theta_{(\ell)} > 0$ with trapped surfaces outside and untrapped surfaces inside.

For isolated MTTs the rate of change of the inward expansion is tied to the surface gravity. To summarize an extended discussion from [25] first note that with a sensible choice of the scaling parameter so that $\mathcal{L}_\ell \theta_{(n)} = 0$, by (5) and (6) we have

$$\kappa_\ell \theta_{(n)} = \mathcal{L}_n \theta_{(\ell)}. \quad (9)$$

With $\theta_{(n)} < 0$, the surface gravity κ_ℓ vanishes if and only if $\mathcal{L}_n \theta_{(\ell)} = 0$. Note that $\mathcal{L}_n \theta_{(\ell)}$ for a spherical MOTS does not depend on the scaling of the null vectors. To see this set $\theta_{(\ell)} = 0$ in (5).

Such time-independent MTTs are *extremal* and we can rewrite this condition in a even more familiar form. Ap-

¹ Except for holographic screens which, though viewed from a different physical perspective, are mathematically identical to marginally trapped tubes.

² For general MOTS things are more complicated as it is necessary to allow for rescaling of the null vectors. We can ignore those complications.

plying the electromagnetic stress energy tensor

$$T_{ab}^{\text{EM}} = \frac{1}{4\pi} \left(F_a{}^c F_{bc} - \frac{1}{4} F_{cd} F^{cd} g_{ab} \right), \quad (10)$$

we find that on a spherical MOTS:

$$\mathcal{L}_n \theta_{(\ell)} = -\frac{1}{r^4} (r^2 - q^2) + 8\pi T_{ab}^{\text{nEM}} \ell^a n^b, \quad (11)$$

where r is the areal radius of the surface, q is the electric charge contained by the surface (we assume the magnetic charge is zero), and T_{ab}^{nEM} is the stress-energy tensor for any non-Maxwell fields. This last term vanishes for some matter fields (including the massless scalar fields and null dust that we will consider later). In these cases

$$\mathcal{L}_n \theta_{(\ell)} \leq 0 \iff \kappa_\ell \geq 0 \iff r \geq q, \quad (12)$$

with the saturation of one bound implying saturation of all the others. For isolated horizons all of the common notions of extremality are equivalent. A spherically symmetric extremal isolated horizon has vanishing surface gravity, no trapped surfaces directly inside and (for the matter models we consider) $r = q$.

For time-dependent MTTs, $\mathcal{L}_\ell \theta_{(n)}$ should not vanish in general and so the vanishing κ_ℓ condition decouples from the other two. Physically this is not surprising as it is not clear how surface gravity should be defined (or even if it can be) for non-stationary spacetimes. That said, the $\mathcal{L}_n \theta_{(\ell)} = 0 \iff r = q$ equivalence remains and it is this dual condition that we will use as a definition of (spherically symmetric) isolated and dynamical extremal horizons. Again see [25] for a more detailed discussion.

Finally note that while we assumed spherical symmetry in showing $r \geq q$ this is actually a much more general bound which holds for all strictly stably outermost MOTS in spacetimes that satisfy the dominant energy condition (including time-dependent cases)[26].

C. Dynamical MTTs: kinematics

In the classification we focussed on time-independent MTTs. We now consider dynamical ones in more detail. First, as long as the radial tangent vector to H is not parallel to n it may be written as

$$\mathcal{V} = \ell - Cn \quad (13)$$

for an expansion parameter C and appropriate scaling of the null vectors [16, 27]. The sign of C determines the signature of H and with $\theta_{(\ell)} = 0$,

$$\theta_{(\mathcal{V})} = -C\theta_{(n)}. \quad (14)$$

Thus for an MTT with:

$C > 0$: H is spacelike and expanding

$C = 0$: H is null (tangent to ℓ) and non-expanding

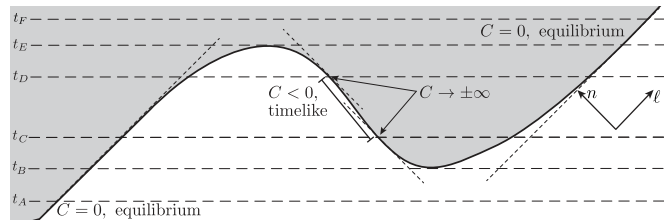


FIG. 1. Cartoon of a smoothly evolving MTT that exhibits an apparent horizon jump (adapted from [28]). The space-time is foliated by a time parameter t . At t_A there is a single isolated horizon in equilibrium with its surroundings. Matter then accretes and the MTT evolves as a spacelike dynamical horizon until t_B where a dense concentration of matter outside the horizon causes a new marginally trapped surface to appear. If one was only tracking outermost marginally trapped surfaces then the apparent horizon would appear to jump at this time. Relative to the time coordinate the new marginally trapped surface bifurcates into a pair of surfaces with one growing and one shrinking. At t_C the inner surface becomes a timelike membrane and remains timelike until t_D when it transitions back to being spacelike. At both of these locations the MTT is parallel to n and C diverges. At t_E we return to a single outer horizon which relaxes to equilibrium at t_F .

$C < 0$: H is timelike and contracting.

Using the language of [19, 20] these are respectively a *dynamical horizon*, a *(weakly) isolated horizon* and a *time-like membrane*. As indicated by the terminology, an isolated horizon represents an equilibrium state. For example all Killing horizons are isolated. If H is tangent to n then by (13), $C = \pm\infty$. We will refer to this as a *null membrane*.

An MTT demonstrating the full range of possible expansion parameters is shown in Figure 1. There the MTT weaves back and forth through a time foliation so that it may intersect a given instant multiple times. From the $(3+1)$ perspective there will then be multiple marginally trapped surfaces at some instants in time (for example t_C and t_D) and for a numerical code tracking only the outermost one as an apparent horizon, the horizon will appear to discontinuously jump (at t_B). If the MTT is spacelike, these multiple horizons may be viewed as resulting from foliation choices (see, for example [29]). However if the MTT has timelike or parallel-to- n null sections there are unambiguous jumps: no foliation choice can remove them (examples may be found in [28, 30])

C depends on the scaling of the null vectors however we can also define an invariant measure of expansion. Following [16, 27] we define an *evolution parameter* ϵ^2 by

$$\frac{\epsilon^2}{r^2} \equiv \frac{1}{2} C \theta_{(n)}^2. \quad (15)$$

Despite the notation, ϵ^2 will be negative if C is negative³. If \mathcal{V} is timelike or spacelike then with respect to $\hat{\mathcal{V}}$, the unit normalized version of \mathcal{V} ,

$$\left| \frac{1}{2} C \theta_{(n)}^2 \right| = \theta_{\hat{\mathcal{V}}}^2. \quad (16)$$

Thus ϵ^2 is the square of the scaled and normalized rate of change of the area with a \pm sign added to indicate whether H is spacelike or timelike.

This parameter vanishes in the isolated limit (even through $\hat{\mathcal{V}}$ itself is not well-defined there). When it is small the MTT is near equilibrium: a *slowly evolving horizon* (see [31] for a range of examples). It diverges for null membranes which, as we have seen, are associated with horizon jumps. Since these are about as far from equilibrium as one could imagine, this is fitting.

D. Marginally trapped tubes: dynamics

We can also consider MTT dynamics. By definition

$$\mathcal{L}_{\mathcal{V}\theta(\ell)} = 0 \iff \mathcal{L}_{\ell\theta(\ell)} - C\mathcal{L}_{n\theta(\ell)} = 0, \quad (17)$$

which for non-degenerate cases (we will return to degenerate cases where $\mathcal{L}_{\ell\theta(\ell)} = \mathcal{L}_{n\theta(\ell)} = 0$ in subsection III C) implies that

$$C = \frac{\mathcal{L}_{\ell\theta(\ell)}}{\mathcal{L}_{n\theta(\ell)}} = \frac{T_{ab}\ell^a\ell^b}{1/(2A) - T_{ab}\ell^an^b}, \quad (18)$$

where $A = 4\pi r^2$. From this expression we can understand how matter drives the evolution of MTTs.

By the null energy condition the numerator is non-negative while the sign of the denominator depends on the stability of the MOTS. The classification is straightforward. First if $T_{ab}\ell^a\ell^b = 0$ then $C = 0$ and we have an isolated horizon. Intuitively this makes sense. $T_{ab}\ell^a\ell^b$ is the flux across a surface with null normal ℓ_a . In this case no matter crosses the horizon and so there is no evolution.

If $T_{ab}\ell^a\ell^b \geq 0$ then the qualitative behaviour of C is determined by the relative size of the stress-energy tensor and the Gaussian curvature of the MOTS:

$1/(2A) > T_{ab}\ell^an^b \Rightarrow C > 0$: H is a dynamical horizon

$1/(2A) = T_{ab}\ell^an^b \Rightarrow C = \pm\infty$: H is a null membrane

$1/(2A) < T_{ab}\ell^an^b \Rightarrow C < 0$: H is a timelike membrane

The first case is the standard one. Infalling matter drives the expansion of the horizon. The second and third are more exotic. There is a shrinking null or timelike membrane like those associated with horizon jumps in Figure 1.

At least for dust spacetimes (Oppenheimer-Snyder or Tolman Bondi) the physical origin of apparent horizon “jumps” is clear[28]. For timelike dust of density ρ moving with four-velocity u^a the stress-energy tensor is

$$T_{ab}^{\text{TD}} = \rho u_a u_b. \quad (19)$$

Then

$$C_{\text{TD}} = \frac{1}{\xi^2} \frac{2\pi r^2 \rho}{1 - 4\pi \rho r^2} \quad (20)$$

where $1/\xi = -2\ell^a u_a$ is a scaling parameter for the null vectors. The denominator is proportional to $\mathcal{L}_{n\theta(\ell)}$ and

$$\mathcal{L}_{n\theta(\ell)} \geq 0 \iff \rho \geq \frac{1}{2A}. \quad (21)$$

Thus there is a dust density threshold set by the inverse horizon area beyond which the dust becomes dense enough to form a new black hole that contains the old one. As seen in FIG. 1, a bubble of untrapped spacetime can remain caught between the old and new apparent horizons but it quickly decays as the timelike membrane approaches and annihilates the inner horizon.

Though this is illustrative and useful in building intuition, timelike dust is not the focus of this paper. Instead we study null dust and (uncharged) scalar fields in a background electromagnetic field. First for (possibly charged) infalling null dust plus an electromagnetic field

$$T_{ab}^{\text{NDEM}} = T_{ab}^{\text{ND}} + T_{ab}^{\text{EM}} = \mu n_a n_b + T_{ab}^{\text{EM}}, \quad (22)$$

so that

$$C_{\text{NDEM}} = \frac{8\pi\mu r^4}{r^2 - q^2}. \quad (23)$$

For charged dust q will be dynamical but for uncharged dust it is constant. Then if $r > |q|$ the expansion will be positive and spacelike while inside $r < |q|$ it will be negative and timelike. We will see this behaviour for outer and inner horizons.

The second type of matter consists of an uncharged scalar field obeying the Klein-Gordon equation

$$\nabla^2 \varphi = m_o^2 \varphi, \quad (24)$$

(where m_o is the mass of the field) along with an electromagnetic field so that

$$T_{ab}^{\text{KGEM}} = \frac{1}{4\pi} \left(\nabla_a \varphi \nabla_b \varphi - \frac{1}{2} (\nabla_c \varphi \nabla^c \varphi + m_o^2 \varphi^2) g_{ab} \right) + T_{ab}^{\text{EM}}. \quad (25)$$

Thus the expansion parameter is

$$C_{\text{KGEM}} = \frac{2r^4 (\mathcal{L}_{\ell\varphi})^2}{r^2 - q^2 - m_o^2 \varphi^2 r^4}, \quad (26)$$

³ The parameter was originally developed for outermost slowly evolving horizons which are always null or spacelike if the energy conditions are satisfied. While we could take the absolute value of this quantity it will be convenient to retain the sign (which will tell us whether the MTT is expanding or contracting).

where q is constant since there is no means of propagating charge in these spacetimes. For a massless scalar field the qualitative evolution is again determined by whether or not a MOTS is outside or inside $r = q$. However for a massive scalar field more complicated evolutions like those in FIG. 1 may be possible⁴.

III. EVOLUTIONS FOR NULL DUST

We now consider our most detailed example. Vaidya Reissner-Nordström spacetimes contain infalling, possibly charged, null dust. In this section we introduce these spacetimes and then use them to study possible exits from extremality along with dynamical extremal horizons.

A. Vaidya Reissner-Nordström and its horizons

1. The spacetime

In Eddington-Finkelstein-like coordinates infalling Vaidya Reissner-Nordström (VRN) spacetimes [32] are described by

$$ds^2 = - \left(1 - \frac{2m(v)}{r} + \frac{q(v)^2}{r^2} \right) dv^2 + 2dvdr + r^2 d\Omega^2 \quad (27)$$

where $m(v)$ and $q(v)$ respectively determine the rate of accretion of mass and charge. The electromagnetic field is defined by the potential

$$A = -\frac{q}{r} dv \quad (28)$$

and the full dust plus electromagnetic stress-energy tensor is

$$T_{ab} = \mu [dv]_a \otimes [dv]_b + T_{ab}^{\text{EM}}, \quad (29)$$

where

$$\mu = \frac{r\dot{m} - q\dot{q}}{4\pi r^3} \quad (30)$$

is the energy density of the dust⁵. The last part, T_{ab}^{EM} is the electromagnetic field stress-energy that is generated by A .

⁴ As far as we know explicit timelike membrane examples have not yet been constructed. An attempt to construct such examples in [28] was not successful though the difficulties obstructing the construction were probably numerical rather than physical.

⁵ Rewriting as

$$\mu = \frac{\dot{m}}{4\pi r^2} - \left(\frac{q}{r} \right) \frac{\dot{q}}{4\pi r^2} \quad (31)$$

this can be seen to have two components: one associated with the dust mass energy and the other with the potential energy of the dust relative to the electromagnetic field.

Note that this stress-energy tensor is consistent with the Maxwell equations which tell us that the electromagnetic field is supported by a (null) current

$$j_{\text{EM}}^b = -\frac{1}{4\pi} \nabla^a F_a{}^b = -\frac{\dot{q}}{4\pi r^2} \left(\frac{\partial}{\partial r} \right)^b. \quad (32)$$

The spacetime satisfies all the standard energy conditions if and only if

$$\dot{m}r - \dot{q}q \geq 0. \quad (33)$$

In particular note that if $q\dot{q} = 0$ then the energy conditions are satisfied as long as $\dot{m} \geq 0$ and so the horizon is expanding as it absorbs positive energy density dust. If $q\dot{q} \neq 0$ then there will always be energy condition violations for

$$r < \left(\frac{\dot{q}}{\dot{m}} \right) q. \quad (34)$$

We will return to these apparent violations in the next subsection and then again in III C.

2. Marginally trapped tubes

As a first step to locating horizons, we define:

$$\ell = \frac{\partial}{\partial v} + \frac{1}{2} \left(1 - \frac{2m}{r} + \frac{q^2}{r^2} \right) \frac{\partial}{\partial r} \quad \text{and} \quad (35)$$

$$n = -\frac{\partial}{\partial r}. \quad (36)$$

Then the geometrical quantities associated with these null vector fields are the expansions

$$\theta_{(\ell)} = \frac{1}{r} \left(1 - \frac{2m}{r} + \frac{q^2}{r^2} \right) \quad \text{and} \quad (37)$$

$$\theta_{(n)} = -\frac{2}{r}, \quad (38)$$

and the inaffinities

$$\kappa_{\ell} = \frac{rm - q^2}{r^3} \quad \text{and} \quad \kappa_n = 0, \quad (39)$$

while the non-zero components of the stress-energy tensor are

$$T_{ab}\ell^a\ell^b = \mu \quad \text{and} \quad (40)$$

$$T_{ab}\ell^a n^b = \frac{q^2}{8\pi r^4}. \quad (41)$$

Thus by (37) there are MTTs at

$$r_{\pm}(v) = m \pm \sqrt{m^2 - q^2}, \quad (42)$$

where r_+ and r_- are the inner and outer horizons. This is exactly the same relation as for regular RN.

Knowing the location of the outer MTT provides some extra insight into the noted violations of the energy condition. Focussing on an extremal horizon ($r_H = m = q$)

such violations will occur outside the horizon when $\dot{q} > \dot{m}$ but otherwise are confined inside. However if $\dot{q} > \dot{m}$ it is also true that an initially extremal horizon would immediately evolve to become a super-extremal naked singularity.

The energy condition violations correspond to the charged dust continuing to move inwards even though the electrical repulsion has become stronger than the gravitational attraction. This last conclusion continues to hold more generally: energy condition violations signal unphysical dust evolution. In Section III C we will examine how this may be corrected but for now assume $\dot{q} < \dot{m}$ to avoid this difficulty for our extremal horizons.

Next consider dynamics of the MTT. From (23) the expansion parameter of these MTTs is

$$C_{\pm} = \pm \left(\frac{r_{\pm} \dot{m} - q \dot{q}}{\sqrt{m^2 - q^2}} \right), \quad (43)$$

where one consistently chooses the positive (minus) signs to get the outer (inner) horizon. By (33), $C_+ \geq 0$ and $C_- \leq 0$: the outer horizon is spacelike (or null) and non-contracting while the inner one is timelike (or null) and non-expanding. For $|q| = m$ this diverges if the numerator is non-zero or is ill-defined if it vanishes. That said, if it immediately exits extremality then we can (and will) study the departure as a limiting process.

The corresponding (scaling invariant) evolution parameter is

$$\epsilon_{\pm}^2 = 2 \left(\dot{m} \pm \frac{m \dot{m} - q \dot{q}}{\sqrt{m^2 - q^2}} \right) \quad (44)$$

and so this invariant parameter also diverges or is ill-defined for extremal horizons. By (42) it can be written in an even simpler form:

$$\epsilon_{\pm}^2 = 2 \dot{r}_{\pm} \quad (45)$$

and so discontinuities in the expansion parameter are equivalent to discontinuities in the rate of change of the areal radius.

B. Exit from equilibrium

Now that we have a concrete (and exactly solvable) model we can study horizon evolutions. We begin with the accretion of uncharged dust onto both extremal and (for comparison) nearly extremal MTTs.

1. Possible exits

Take a black hole with initial charge q_o and mass $m_o \geq |q_o|$ and without loss of generality assume the accreting dust first crosses the horizon at $v = 0$ (so $m = m_o$ and $q = q_o$ for $v \leq 0$). We are interested in the transition

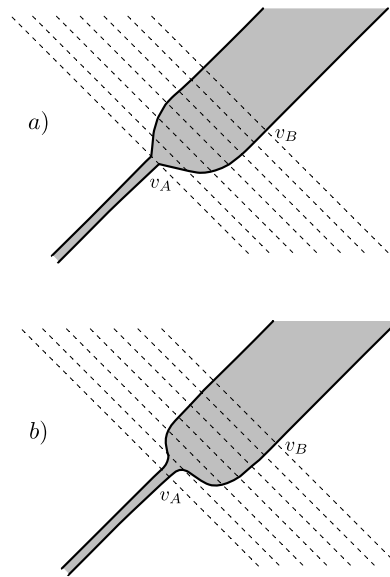


FIG. 2. Evolution of an initially non-extremal RN horizon. The trapped region is shaded and null directions are at 45° to the horizontal as in FIG. 1. The accreting dust begins crossing the horizon at $v = v_A$ and finishes at v_B . It is represented by dashed lines. a) represents the $k = 1$ case where the rate of expansion jumps discontinuously to a finite value as the first matter arrives while for b) $k > 1$ the rate is continuous. In both cases the inner MTT becomes timelike while the outer MTT becomes spacelike.

from equilibrium and so expand $m(v)$ as a Taylor series and consider only the leading term. Thus for a time scale v_o and $0 \leq v \ll v_o$:

$$m(v) = m_o \left(1 + (v/v_o)^k + O\left(\frac{v}{v_o}\right)^{k+1} \right) \quad (46)$$

for some positive integer k .

For such a mass function the evolution parameter takes different forms for non-extremal versus initially extremal horizons. For $0 \leq v \ll v_o$, (45) gives:

$$\epsilon_{\pm}^2 \approx \begin{cases} \frac{2km}{v_o} \left(1 \pm \frac{1}{\sqrt{1-(q_o/m_o)^2}} \right) \left(\frac{v}{v_o} \right)^{k-1} & q_o < m_o \\ \pm \left(\frac{\sqrt{2}km_o}{v_o} \right) \left(\frac{v}{v_o} \right)^{k/2-1} & q_o = m_o \end{cases} \quad (47)$$

so the details of transitions are determined by the limits of these expressions as $v \rightarrow 0$.

Focussing first on the non-extremal horizon there are two classes of transition from isolation:

$$\lim_{v \rightarrow 0} \epsilon_{\pm}^2|_{\text{non ex}} = \begin{cases} \frac{2m}{v_o} \left(1 \pm \frac{1}{\sqrt{1-(q_o/m_o)^2}} \right) & k = 1 \\ 0 & k > 1 \end{cases}. \quad (48)$$

For $k > 1$ the evolution parameter changes continuously as the matter arrives but for $k = 1$ (a linear increase in mass) the evolution parameter jumps discontinuously.

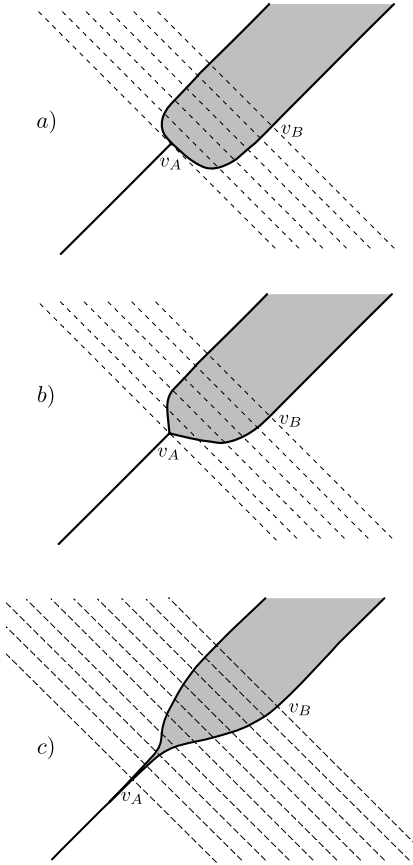


FIG. 3. Evolution of an initially extremal RN horizon. Diagrams are set up in the same way as in FIG. 2. Respectively they are a) $k = 1$, b) $k = 2$ and c) $k > 2$.

Instantaneously the inner and outer horizons become a timelike membrane and a dynamical horizon. However, this discontinuity is not really a surprise since by (30) there is also a discontinuity in the Ricci tensor⁶. The two possibilities are depicted schematically in FIG. 2.

For an initially extremal horizon things are more interesting. The evolution parameter is

$$\lim_{v \rightarrow 0} \epsilon_{\pm}^2|_{\text{ex}} = \begin{cases} \pm\infty & k = 1 \\ \pm \frac{2\sqrt{2}m_o}{v_o} & k = 2 \\ 0 & k \geq 3 \end{cases}. \quad (49)$$

This time there are three characteristic evolutions from extremality which are depicted schematically in FIG. 3.

⁶ This discontinuity is physically caused by the jump of the dust energy density from zero to a finite value at $v = 0$. It is not caused by the presence of a thin shell discontinuity (null or otherwise). By the junction conditions for null surfaces ([33–35] or [36] for a textbook presentation) the energy density of any such shell at $v = 0$ would be proportional to the jump in the inner expansion $\theta_{(n)}$. This is zero by (38). The pressure in such a shell would be proportional to the jump in κ_ℓ . This is also zero by (39).

For $k = 1$ the arrival of matter causes the MTT to jump from being isolated and parallel to ℓ to being maximally evolving and parallel to n . For $k = 2$ the situation is analogous to the $k = 1$ case for non-extremal horizons: the jump is discontinuous to a timelike inner and space-like outer MTT. However in this case the Ricci tensor is continuous and the discontinuity instead follows from the extremality. Finally for $k \geq 3$, the evolution parameter is continuous.

Regardless of the details, in all three of these cases we have a tripartite MTT: the initially extreme horizon splits into two non-extremal pieces which remain distinct. However for the extremal $k = 1$ case we can also recognize a more familiar situation if we temporarily disregard the initial state: the timelike membrane and dynamical horizon connect at an instantaneous null membrane. This is similar to the behaviour observed during horizon jumps.

2. Complete evolutions

Informed by these observations we can also consider full evolutions which include a return to equilibrium. As before we fix $q = q_o$ and now consider piecewise mass functions of the form

$$m(v) = \begin{cases} m_o & v < 0 \\ m_o(1 + m_\Delta \mu(v)) & 0 \leq v \leq 1 \\ m_o(1 + m_\Delta) & v > 1 \end{cases}, \quad (50)$$

where μ is a continuous function with $\mu(0) = 0$ and $\mu(1) = 1$. Thus $m(v)$ is similarly continuous though not necessarily differentiable. For such mass functions the initial and final areal radii of the inner and outer horizon are respectively

$$r_o^\pm = m_o \pm \sqrt{m_o^2 - q_o^2} \quad \text{and} \quad (51)$$

$$r_f^\pm = (m_o + m_\Delta) \pm \sqrt{(m_o + m_\Delta)^2 - q_o^2}. \quad (52)$$

Our examples take near-extremal $q_o = 0.999m_o$ and extremal $q_o = m_o$ horizons as initial states. We take $m_\Delta = m_o/20$ and consider three increasingly smooth $\mu(v)$:

$$\mu_1 = v \quad (53)$$

$$\mu_2 = -v^2(2v - 3)$$

$$\mu_3 = v^3(6v^2 - 15v + 10)$$

The subscript indicates at which order of derivative the full m becomes discontinuous. Thus for μ_1 , the first derivative of the mass function is discontinuous at $v = 0$ and $v = 1$, while for μ_3 the discontinuity doesn't show up until the third order derivative.

These MTTs and the corresponding expansion parameters are plotted in FIG. 4. The expected discontinuities from the earlier analysis are seen: for the initially extremal case there is an infinite discontinuity for $k = 1$ and finite for $k = 2$ while for non-extremal there is only a

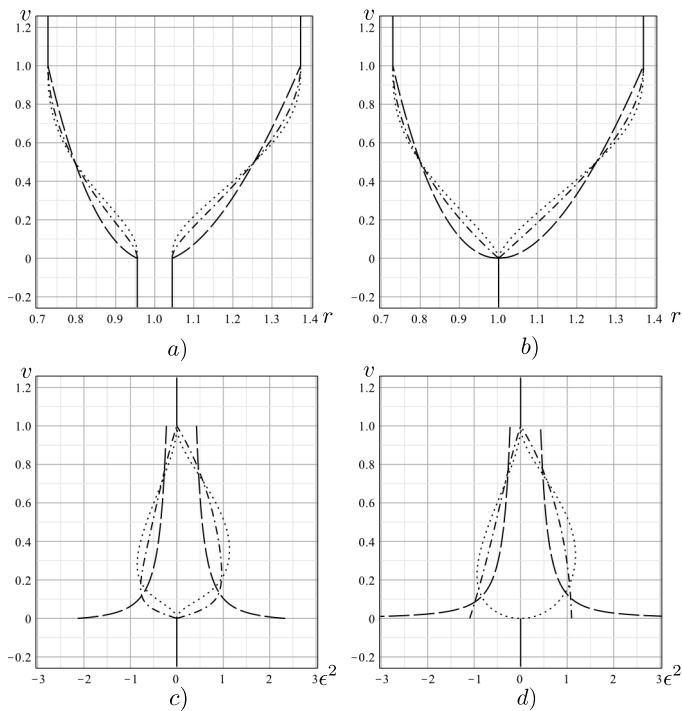


FIG. 4. Inner and outer horizon evolutions for a) near extremal ($q_o = 0.999m_o$) and b) extremal ($q_o = m_o$) VRN spacetimes. In both cases the areal radius r is on the horizontal axis and Eddington-Finkelstein time v on the vertical (both in units of m_o). Below these subfigures, c) and d) plot the corresponding evolution parameters. In all four subfigures the different curves represent accreting matter of varying degrees of smoothness. Long dashes are μ_1 , dot-dashes μ_2 and dots μ_3 . When all models behave in the same way a solid black line is used.

finite discontinuity for $k = 1$. At the other end of the evolution ($v = 1$) there are discontinuities in the evolution parameter for $k = 1$ (again reflecting the corresponding discontinuity in the Ricci tensor) while for higher k it returns to equilibrium continuously.

C. Evolution at extremality

With the accretion of matter the MTTs of the last section immediately became non-extremal. In this subsection we consider another case: the MTTs remain extremal throughout their evolution. Such evolutions are generated by $q(v) = m(v)$ dust accreting onto an extremal horizon. With this matter, the energy conditions require

$$\dot{m}r - \dot{q}q = \dot{m}(r - m) \geq 0 \text{ for } r \geq m. \quad (54)$$

The horizon of an extremal VRN is at $r_{\text{ex}} = m$ and so, as shown in FIG. 5a) the energy conditions hold on and outside the horizon. What happens inside is a bit more complicated.

For VRN spacetimes where the corresponding violations occur outside the horizon it has been argued by Ori [37] that they are indicative of regions where the solution is no longer physically meaningful. They occur in regions where the electromagnetic repulsion has become stronger than the gravitational attraction yet the solution still requires the dust to move inwards. Ori resolved this physical inconsistency by surgically removing the problematic region and replacing it with an outgoing VRN spacetime matched across the transitional region. Then the newly constructed solution described a shell that fell inwards until the electromagnetic repulsion caused it to bounce back outwards. In that paper careful physical arguments are used to motivate this construction.

In this section we will implement a similar resolution for extremal VRN. In preparation for this we review outgoing VRN.

1. Outgoing VRN

Just as the ingoing VRN metric closely resembles Reissner-Nordström in ingoing Eddington-Finkelstein coordinates, so does the outgoing VRN metric resemble Reissner-Nordström in outgoing Eddington-Finkelstein coordinates:

$$ds^2 = - \left(1 - \frac{2M(u)}{r_{\text{out}}} + \frac{Q(u)^2}{r_{\text{out}}^2} \right) du^2 - 2du dr_{\text{out}} + r_{\text{out}}^2 d\Omega. \quad (55)$$

This time u labels the outgoing radial null geodesics. r_{out} is again the areal radius of spherical shells however we add the subscript to emphasize that $\partial/\partial r_{\text{out}}$ is a very different vector than it is for ingoing Vaidya (in particular it is future-outward rather than past-outward pointing). As is the case for RN in these coordinates, this version of VRN describes a white hole.

The spacetime satisfies all of the energy conditions if and only if

$$QQ' - r_{\text{out}}M' \geq 0, \quad (56)$$

where derivatives with respect to u are indicated by primes. Note that if $QQ' = 0$ we must have M non-increasing and so the white hole shrinks as it emits positive energy dust. If $QQ' \neq 0$ and $M' < 0$ then there will always be energy condition violations for

$$r_{\text{out}} < \left| \frac{Q'}{M'} \right| Q. \quad (57)$$

This is all depicted (for the extremal case) in FIG. 5b).

Turning to geometry and horizons, a suitable pair of outward and inward future null vectors are

$$\ell = \frac{\partial}{\partial r_{\text{out}}} \text{ and } \quad (58)$$

$$n = \frac{\partial}{\partial u} - \frac{1}{2} \left(1 - \frac{2M}{r_{\text{out}}} + \frac{Q^2}{r_{\text{out}}^2} \right) \frac{\partial}{\partial r_{\text{out}}}, \quad (59)$$

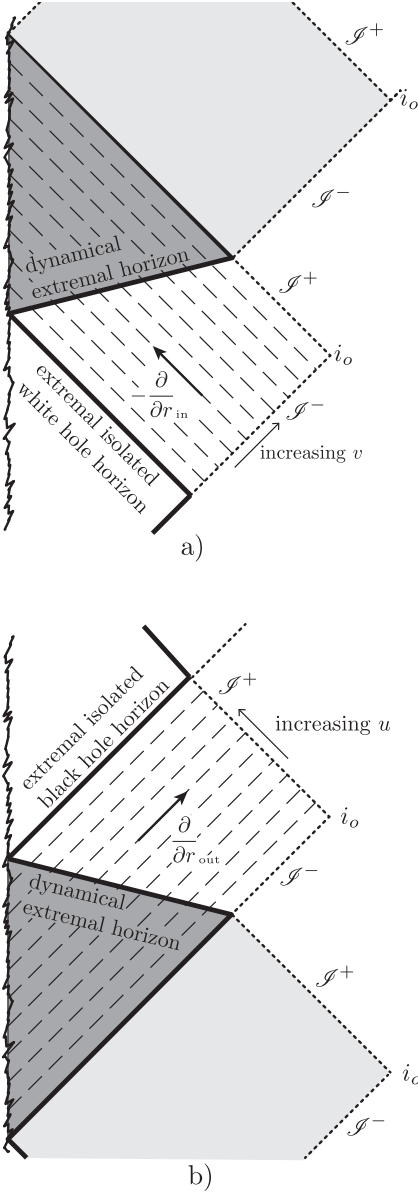


FIG. 5. Extremal dynamical Vaidya spacetimes. In a) infalling Vaidya, $\dot{q} = \dot{m}$ dust falls through the black hole horizon causing it to expand as a spacelike surface. In b) outgoing Vaidya, $\dot{q} = \dot{m}$ dust is emitted from a white hole horizon causing it to shrink, again as a spacelike surface. In both cases regions that will be excised in the construction of FIG. 6 are shaded in (light or dark) gray. The region where the energy conditions are violated is shaded darker and there the dust continues to move inwards (or outwards) even though the electromagnetic force acting on the dust is stronger than the gravitational one.

which have expansions

$$\theta_{(\ell)} = \frac{2}{r_{\text{out}}} \quad \text{and} \quad (60)$$

$$\theta_{(n)} = -\frac{1}{r_{\text{out}}} \left(1 - \frac{2M}{r_{\text{out}}} + \frac{Q^2}{r_{\text{out}}^2} \right). \quad (61)$$

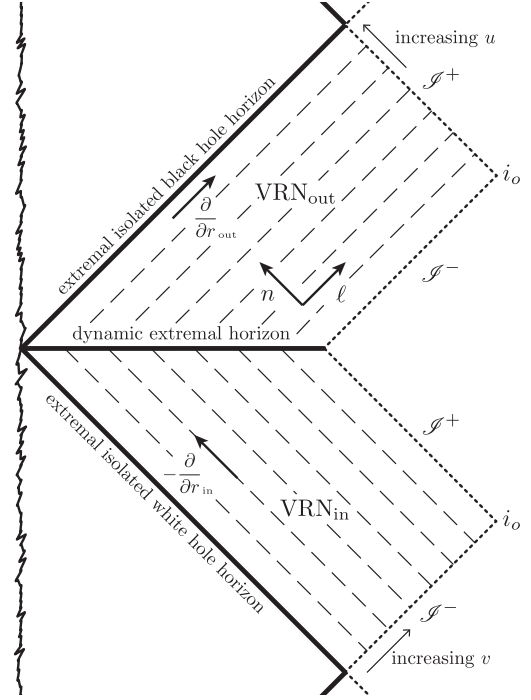


FIG. 6. A Carter-Penrose diagram of an extremal RN black hole irradiated with extremal null dust. VRN_{in} is a region of ingoing VRN where dust accretes onto the black hole while VRN_{out} is a region of outgoing VRN where a white hole radiates dust. They meet on a common MTT which is dynamical and spacelike. The jagged line represents the timelike singularity at $r = 0$ while the dotted outer lines are future and past null infinities. Note that there are no trapped regions.

In this case the *inward* expansion vanishes at

$$r_{\pm\text{out}}(u) = M(u) \pm \sqrt{M(u)^2 - Q(u)^2}, \quad (62)$$

and between these roots spacetime is anti-trapped (both expansions are positive). Of course for an extremal RN solution, this anti-trapped region vanishes.

The non-zero components of the stress-energy tensor also take a similar form to that for infalling VRN:

$$T_{ab}\ell^a n^b = \frac{Q^2}{8\pi R^4} \quad \text{and} \quad (63)$$

$$T_{ab}n^a n^b = \frac{QQ' - RM'}{4\pi R^3}. \quad (64)$$

2. Matching infalling to radiating extremal VRN

We are now ready to construct our dynamical extremal VRN spacetime. Respectively we set $q = m$ and $Q = M$ and assume that that $\dot{m} > 0$ and $M' < 0$ at all times so that the MTTs at $r_{\text{in}} = m$ and $r_{\text{out}} = M$ are always spacelike (this simplifies the construction). Then as shown in FIG. 5 for $r_{\text{in}} < m$ and $r_{\text{out}} < M$ the energy conditions are violated in both spacetimes. We excise those regions and connect the remaining sections of the spacetime along the

extremal MTT as shown in FIG. 6. We can analyze this connection by checking the usual junction conditions: in this case for spacelike surfaces [33–36, 38].

Starting with the infalling (black hole) side of the geometry we parameterize the MTT with induced coordinates $y_{\text{in}}^i = \{v, \theta, \phi\}$ (note the use of mid-alphabet latin indices to indicate we are referring to the MTT). Then the MTT three-metric is

$$h_{ij}^{\text{in}} dy_{\text{in}}^i dy_{\text{in}}^j = 2\dot{m} dv^2 + m^2 d\Omega^2. \quad (65)$$

As expected for $\dot{m} \geq 0$ this is spacelike. Correspondingly for the radiating (white hole) side we parameterize the MTT with induced coordinates $y_{\text{out}}^i = \{u, \theta, \phi\}$ and find the three-metric is

$$h_{ij}^{\text{out}} dy_{\text{out}}^i dy_{\text{out}}^j = -2M' du^2 + M^2 d\Omega^2. \quad (66)$$

For $M' < 0$ this is spacelike.

We can match the ingoing and outgoing spacetimes induced metrics on the MTT, with the (on MTT) coordinate transformation

$$u = -v \quad (67)$$

and choosing

$$M(u) = m(v) = m(-u). \quad (68)$$

The apparently opposite arrows of time on either side of the MTT are okay. Keep in mind that these are just the induced coordinates on a spacelike surface. Thus if the associated coordinate vectors point in opposite directions this is not physically significant.

For comparison with the earlier cases, the expansion parameter may be found kinematically from the tangent vector to the common horizon. Respectively on the ingoing and outgoing sides:

$$\mathcal{V} = \frac{\partial}{\partial v} + \dot{m} \frac{\partial}{\partial r} = \frac{\partial}{\partial r} - m' \frac{\partial}{\partial u}, \quad (69)$$

so

$$C = \dot{m} \quad (70)$$

and

$$\epsilon^2 = 2\dot{m}. \quad (71)$$

Thus as we already saw in (65) and (66) the common horizon is spacelike. This is the same as for non-extremal evolution and as before there will be a (finite) discontinuity in the evolution parameter if the derivative of the mass function is also discontinuous.

Unfortunately, a thin shell singularity is imposed by this matching. We calculate this by first finding the extrinsic curvatures of the MTT. It is most convenient to calculate and express them with respect to a tetrad tied

to the geometry of the horizon. In the two coordinate systems we have

$$\hat{e}_{(0)} = \frac{1}{\sqrt{2\dot{m}}} \frac{\partial}{\partial v} - \sqrt{\frac{\dot{m}}{2}} \frac{\partial}{\partial r_{\text{in}}} = \frac{1}{\sqrt{2\dot{m}}} \frac{\partial}{\partial u} + \sqrt{\frac{\dot{m}}{2}} \frac{\partial}{\partial r_{\text{out}}} \quad (72)$$

$$\hat{e}_{(1)} = \frac{1}{\sqrt{2\dot{m}}} \frac{\partial}{\partial v} + \sqrt{\frac{\dot{m}}{2}} \frac{\partial}{\partial r_{\text{in}}} = \frac{-1}{\sqrt{2\dot{m}}} \frac{\partial}{\partial u} + \sqrt{\frac{\dot{m}}{2}} \frac{\partial}{\partial r_{\text{out}}} \quad (73)$$

$$\hat{e}_{(2)} = \frac{1}{m} \frac{\partial}{\partial \theta} \quad (74)$$

$$\hat{e}_{(3)} = \frac{1}{m \sin \theta} \frac{\partial}{\partial \theta}. \quad (75)$$

where \hat{e}_0 is the future-oriented unit timelike normal, \hat{e}_1 is the outward-pointing unit radial vector (tangent to the MTT) and $\hat{e}_{(2)}$ and $\hat{e}_{(3)}$ are the unit angular vectors. In the usual way the corresponding one-forms will be written with raised tetrad labels: $\hat{e}^{(0)}$, $\hat{e}^{(1)}$, $\hat{e}^{(2)}$ and $\hat{e}^{(3)}$.

Then the extrinsic curvatures $K_{(i)(j)} = \hat{e}_{(i)}^a \hat{e}_{(j)}^b \nabla_a \tilde{e}_b^{(0)}$ (i and j only run from 1 to 3) for the infalling (accreting) and outward radiating sides are

$$K^{\text{in}} = -\frac{\ddot{m}}{(2m)^{3/2}} (\hat{e}^{(1)} \otimes \hat{e}^{(1)}) - \frac{1}{m} \sqrt{\frac{\dot{m}}{2}} (\hat{e}^{(2)} \otimes \hat{e}^{(2)} + \hat{e}^{(3)} \otimes \hat{e}^{(3)}) \quad (76)$$

and

$$K^{\text{out}} = \frac{\ddot{m}}{(2m)^{3/2}} (\hat{e}^{(1)} \otimes \hat{e}^{(1)}) + \frac{1}{m} \sqrt{\frac{\dot{m}}{2}} (\hat{e}^{(2)} \otimes \hat{e}^{(2)} + \hat{e}^{(3)} \otimes \hat{e}^{(3)}). \quad (77)$$

That is $K^{\text{in}} = -K^{\text{out}}$ and so there will be a thin shell singularity along the MTT.

This seems to contradict [37] where for the non-extremal cases it was stated (but not shown) that the extrinsic curvatures match and so there is no thin shell. However in our extreme case, the negative sign is quite intuitive. By (67) and (68) the two sides of the MTT are time-reversed images of each other and so it is not surprising that the extrinsic curvatures, which are essentially time derivatives of the intrinsic metric, have opposite signs.

We can then calculate the form of the stress-tensor for that thin shell:

$$S_{ij} = -\frac{1}{8\pi} ((K_{ij}^{\text{out}} - K_{ij}^{\text{in}}) - (K^{\text{out}} - K^{\text{in}}) h_{ij}). \quad (78)$$

That is

$$S = -\frac{1}{2\pi m} \sqrt{\frac{\dot{m}}{2}} (\hat{e}^{(1)} \otimes \hat{e}^{(1)}) - \frac{m\ddot{m} + 2\dot{m}^2}{4\pi m(2\dot{m})^{3/2}} (\hat{e}^{(2)} \otimes \hat{e}^{(2)} + \hat{e}^{(3)} \otimes \hat{e}^{(3)}). \quad (79)$$

Thus there is instantaneous stress at the transition. If $\dot{m} = 0$ it is an isotropic (negative) pressure otherwise it is anisotropic.

Note however that this stress is strangely innocuous. By (40), (41), (64) and (63) the bulk part of the stress-energy tensor is continuous across the MTT: there are no lasting jumps in either energy, momentum or stress density. This may seem surprising given the appearance of FIG. 6 (and the fact that the electric current (32) certainly does discontinuously change direction there). The root of this behaviour can be found in (40) and (64) which both vanish on the MTT. The mass-energy density of the dust is exactly balanced by the (negative) electromagnetic potential energy on the MTT (see the discussion in footnote 5) and so the net flow of mass-energy vanishes at the MTT.

These results can be cross-checked from a direct analysis of the junction conditions. Following [34] the change in momentum of the matter across the shell is

$$\hat{e}_{(k)}^a (T_{ab}^{\text{out}} - T_{ab}^{\text{in}}) \hat{e}_{(0)}^b = \hat{e}_{(k)}^j D_i S^i_j \quad (80)$$

where D_i is the covariant derivative compatible with h_{ij} . We have already noted that the left-hand side vanishes but one can also directly calculate the right-hand side using (65) and (79) and find that it also vanishes (as it should). Similarly the change in the energy density across the shell is

$$(T_{ab}^{\text{out}} - T_{ab}^{\text{in}}) \hat{e}_{(0)}^a \hat{e}_{(0)}^b = \frac{1}{2} (K_{ij}^{\text{in}} + K_{ij}^{\text{out}}) S^{ij}. \quad (81)$$

Above we noted that there is no change in energy density and this can easily be confirmed on the right-hand side since $K_{ij}^{\text{in}} = -K_{ij}^{\text{out}}$.

Thus while there is a thin-shell singularity imposed by the matching, it does not appear to have any dramatic physical impact. One might speculate that this is what happens when (not-very-physical) charged null dust turns around: it is not the cause of the change in direction but rather the effect. This deserves some further investigation, especially in light of the tension with [37] which did not find a thin shell in non-extremal cases, however that is beyond the scope of this paper and will be left for a future investigation.

Finally, before leaving this spacetime we note the following features. As can be seen in FIG. 6 the inner MTT remains forever null and isolated. No matter ever reaches that surface but instead is bounced back out by the combined electric charge of the original black hole and accreted charged dust. Further there are no trapped (or anti-trapped) surfaces anywhere in this spacetime.

IV. EVOLUTIONS FOR SCALAR FIELDS

We now consider how a massless and uncharged scalar field drives the evolution of initially extremal RN horizons. While spacetimes with scalar fields are not exactly solvable, they have been extensively studied both numerically and analytically.

Most recently much of this interest has focussed on extremal instabilities. While the initial work was in the test

field approximation, Murata, Reall and Tanahashi [15] (henceforth MRT) have numerically studied the evolution of spherically symmetric scalar fields around an initially extremal RN black holes in massless Klein-Gordon Maxwell-Einstein theory. We will compare our results to that paper.

A. Evolution from extremal MTTs

For a massless scalar field, (26) gives:

$$\epsilon^2 = \frac{8r^4 (\mathcal{L}_\ell \varphi)^2}{r^2 - q^2}, \quad (82)$$

where q is constant since there is no means of propagating charge in these spacetimes. Evolutions are driven by non-zero $\mathcal{L}_\ell \varphi$ and we can apply the intuition gained for null dust to understand the possibilities here.

We begin with non-extremal MTTs. As usual we have $r \geq q$ for a strictly stably outermost MOTs with $r = q$ for extremality ($\mathcal{L}_n \theta_{(\ell)} = 0$). A subextremal MTT will then be null and isolated if $\mathcal{L}_\ell \varphi = 0$ and otherwise be dynamical, spacelike and expanding. Correspondingly inner horizon MTTs (which are in some sense superextremal) will be null and isolated if $\mathcal{L}_\ell \varphi = 0$ and otherwise contracting timelike membranes. Thus any evolution should further separate the geometric horizons and drive the black hole farther away from extremality.

Departures from extremality should be very similar to those which we explored for Vaidya RN. The value of the initial expansion will depend on the limiting value of C : in principle it could be zero, finite or infinite depending on how quickly $\mathcal{L}_\ell \varphi$ departs from zero. However whatever the details, the extremal MTT splits to become an inner timelike membrane and outer dynamical horizon as in the schematic FIG. 3.

At least for the outer MTT this is in accord with the observations of MRT. In their paper they study the evolution of both outgoing and ingoing scalar wave packets and find that generically in both cases the outer horizon settles down to a non-extreme black hole. This agrees with our conclusions from (26). If $\mathcal{L}_\ell \varphi \neq 0$ at any time then the horizon will exit extremality. For the inner horizon things are a bit more complicated as there are other potential instabilities there. Dealing with these are beyond the scope of the current paper and we refer the reader to MRT for a detailed discussion (including evidence that dynamic inner horizons are actually more stable than time-independent ones).

Returning to the outer MTT, keep in mind that since these matter fields cannot carry charge, q will remain constant throughout any evolution. Thus dynamical extremal MTTs like those discussed in the previous section are impossible for these spacetimes.

B. Dynamically extremal event horizons

However there is an alternate notion of extremality based on causal rather than geometric horizons. A black hole spacetime can be said to be extremal if the event horizon contains no trapped surfaces[1].

For finely tuned outgoing scalar wave packets, MRT construct examples of such event horizons. In their examples, the scalar field accretes onto a charged central singularity so that the spacetime asymptotically approaches extremal RN. They show that there are no trapped surfaces anywhere in this spacetime and so the event horizon may be considered dynamically extremal.

These spacetimes also do not contain any spherical MOTS. This follows from: i) for any MOTS $r_{\text{MOTS}} \geq q$ [26], ii) MOTS are necessarily inside event horizons, iii) in these spacetimes the event horizon only approaches q asymptotically (from below) and (iv) the expansion $\theta_{(n)}$ of the ingoing radial null geodesics is negative. Thus all surfaces of constant r in the casual future of the event horizon have $r < q$ and so cannot be MOTS.

To get a better intuition for the structure of these dynamically extremal event horizon spacetimes let us return to our much simpler null dust spacetimes and consider the analogous situation there. This will also help to motivate a further property of these spacetimes: they contain naked singularities.

Fix $\dot{q} = 0$, $m \leq q$ and $\lim_{v \rightarrow \infty} m = q$. Then there are two possibilities depending on whether or not the limit is achieved. In FIG. 7a) $m(v)$ asymptotes towards q but doesn't achieve its limit. Thus no MOTS forms but there is still an event horizon: the null surface that asymptotes to $r = q$ as $v \rightarrow \infty$. FIG. 7b) achieves the limit at finite v at which point we switch $\dot{m} = 0$. Beyond that point there is an extremal isolated MOTS and this can be evolved backwards to find the full event horizon. Note that in both cases there is a singularity which is visible both inside and outside the horizon.

In fact we argue that such naked singularities are not a special property of the null dust spacetimes but are generic for dynamically extremal black hole spacetimes which are charged but have no charge carrying field (and so are also present in MRT). In such a spacetime, there is always a singularity at $r = 0$ (thanks to the unchanging non-zero electric charge at the origin) and so the only question is whether the event horizon can fully clothe that singularity. It can't: the Raychaudhuri equation along with the null energy condition implies that all outward moving null shells (this includes any event horizon) necessarily emerge from the origin. Null rays outside the event horizon also originate from the singularity and so it is visible to observers at infinity.

It is unclear whether or not naked singularities are a generic feature of dynamically extremal event horizon spacetimes. If one allows other charge carrying matter fields to be active in the past during the formation of the singularity, then clothing might be possible. However even if that is not the case (it seems likely that electrical

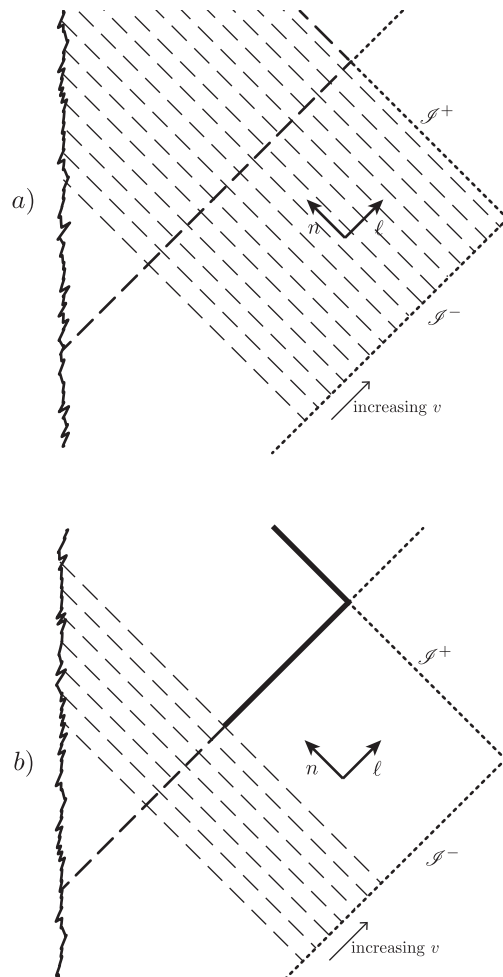


FIG. 7. Finely tuned evolution of an initially naked singularity into an extremal black hole for null dust spacetimes. Long dashed lines are event horizons while heavy solid lines are MTTs. Subfigure a) is in the spirit of [15] with neither trapped nor marginally trapped surfaces. In this case $m(v) < m_o$ throughout but $\lim_{v \rightarrow \infty} m(v) = m_o$. However in subfigure b) the limit is achieved and so a MOTS forms. In both cases there is a naked singularity.

repulsion would forbid the formation of a $q > m$ singularity even if charge carrying fields are allowed) for a different choice of matter fields naked singularities might be avoidable.⁷

⁷ A scenario for the construction of such a spacetime might follow from an example by Williams [39]. For carefully chosen massive scalar field characteristic initial data representing the interior of a black hole (one of the null surfaces is the event horizon) she demonstrated that there could be no (spherically symmetric) MTT asymptotic to any event horizon. This implies that there are also no (spherically symmetric) trapped surfaces close to the event horizon. Thus such a spacetime would be at least locally extremal in the sense of [1]. Note however that her construction neither excludes the possibility of trapped surfaces deeper inside the black hole nor a naked singularity in the causal past. How-

V. DISCUSSION

We have seen that geometric VRN horizons evolving from extremality demonstrate several interesting behaviours.

First, they are tripartite. When matter accretes onto an extremal MTT it bifurcates into a pair of MTTs: an inner and an outer horizon. While this is physically expected, it is something that does not happen during generic black hole evolutions. In $(3+1)$ general relativity it has been shown that strictly stably outermost MOTS on one slice necessarily evolve uniquely into MOTS on future slices[23, 40]. However it is clear that the spacetimes depicted in FIG. 3 can be foliated so that a single horizon does evolve into two. There is no contradiction: isolated extremal horizons are not strictly stably outermost.

In FIG. 7 we saw another example of an unexpected behaviour: an extremal marginally trapped tube forming instantaneously. Again this isn't usually seen for marginally trapped tubes which may weave backwards and forwards through spacetime but do not generally appear out of nowhere. During gravitational collapse they may appear out of the central singularity as it forms and there are known examples of them forming out of or disappearing into shockwave singularities [41] however as far as we know this kind of appearance “from thin air” has not been commented on before. Once more the strangely behaving horizon is extremal and so not subject to the usual theorems for strictly stably outermost horizons. With this perspective it is not so different from apparent horizon “jumps” like the one depicted at t_B in FIG. 1. There it is also the case that $\mathcal{L}_{\hat{r}}\theta_{(\ell)} = 0$ at the moment of appearance (where \hat{r}^a is the radial tangent to the slice).

The transition from isolation can be more dramatic than that for a non-extremal horizon. Linear ($k = 1$) accretion will cause a kink in the horizon and jump in the evolution parameter for any MTT (there is a corresponding discontinuity in the density of accreting matter) however for an initially extremal horizon it generates an instantaneous transition to a null membrane (with

$\epsilon^2 = \pm\infty$). Even with a continuous matter distribution there can be kinks in the MTT (for $k = 2$ matter). The extremality introduces an extra level of possible discontinuity due to the form of the expansion parameter (43). Similar results follow for transitions driven by scalar fields.

We also examined two notions of dynamical extreme spacetimes. The first was for a dynamic extremal MTT. There infalling $q = m$ matter generates a pair of extremal MTTs (one isolated and the other dynamic). Constructing these examples in exact form required the careful use of spacetime surgery to connect ingoing and outgoing Vaidya solutions. While the bulk part of the stress-energy tensor is continuous across the junction, the extrinsic curvatures on the two sides of the junction do not match (they differ by a negative sign) and so an instantaneous thin shell of matter makes an appearance along the junction. Its physical significance is not entirely clear and deserves further investigation. While these evolutions are of doubtful physical importance being both finely tuned and driven by unrealistic matter, they remain as interesting examples of possible behaviours that are not forbidden by the energy conditions.

The second notion of dynamical extremality, proposed in [15], is a spacetime with an event horizon but no trapped or even marginally trapped surfaces. We considered such situations for null dust spacetimes and saw that they contain naked singularities. From more general considerations it also appears that any other such spacetime with a fixed central electric charge will be nakedly singular. In such spacetimes dynamical extreme event horizons emerge from naked singularities. However we also noted that for other matter fields this may not be the case.

ACKNOWLEDGEMENTS

Thanks to Hari Kunduri and Andrey Shoom for useful discussions about this work and Harvey Reall for his comments on an earlier version of this paper. IB was supported by NSERC Discovery Grant 261429-2013.

-
- [1] Werner Israel, “Third law of black-hole dynamics: A formulation and proof,” *Phys. Rev. Lett.* **57** (1986).
 - [2] Andrew Strominger and Cumrun Vafa, “Microscopic origin of the Bekenstein-Hawking entropy,” *Phys.Lett.* **B379**, 99–104 (1996), arXiv:hep-th/9601029 [hep-th].
 - [3] Jorg Hennig, Marcus Ansorg, and Carla Cederbaum, “A Universal inequality between angular momentum and horizon area for axisymmetric and stationary black

holes with surrounding matter,” *Class. Quant. Grav.* **25**, 162002 (2008), arXiv:0805.4320 [gr-qc].

- [4] Marc Mars, “Stability of MOTS in totally geodesic null horizons,” *Class. Quant. Grav.* **29**, 145019 (2012), arXiv:1205.1724 [gr-qc].
- [5] Jose Luis Jaramillo, Martin Reiris, and Sergio Dain, “Black hole Area-Angular momentum inequality in non-vacuum spacetimes,” *Phys.Rev.* **D84**, 121503 (2011), arXiv:1106.3743 [gr-qc].
- [6] Maria E. Gabach Clement, Jose Luis Jaramillo, and Martin Reiris, “Proof of the area-angular momentum-charge inequality for axisymmetric black holes,” *Class. Quant. Grav.* **30**, 065017 (2013), arXiv:1207.6761 [gr-qc].

ever, it at least seems possible in principle that such an event horizon could fully clothe a central singularity that formed at finite time.

- [7] Jerzy Lewandowski and Tomasz Pawłowski, “Extremal isolated horizons: A Local uniqueness theorem,” *Class.Quant.Grav.* **20**, 587–606 (2003), arXiv:gr-qc/0208032 [gr-qc].
- [8] Hari K. Kunduri and James Lucietti, “Classification of near-horizon geometries of extremal black holes,” *Living Rev.Rel.* **16**, 8 (2013), arXiv:1306.2517 [hep-th].
- [9] Stefanos Aretakis, “Stability and Instability of Extreme Reissner-Nordström Black Hole Spacetimes for Linear Scalar Perturbations I,” *Commun.Math.Phys.* **307**, 17–63 (2011), arXiv:1110.2007 [gr-qc].
- [10] Stefanos Aretakis, “Stability and Instability of Extreme Reissner-Nordstrom Black Hole Spacetimes for Linear Scalar Perturbations II,” *Annales Henri Poincaré* **12**, 1491–1538 (2011), arXiv:1110.2009 [gr-qc].
- [11] Stefanos Aretakis, “A note on instabilities of extremal black holes under scalar perturbations from afar,” *Class.Quant.Grav.* **30**, 095010 (2013), arXiv:1212.1103 [gr-qc].
- [12] Stefanos Aretakis, “Horizon Instability of Extremal Black Holes,” (2012), arXiv:1206.6598 [gr-qc].
- [13] James Lucietti and Harvey S. Reall, “Gravitational instability of an extreme Kerr black hole,” *Phys.Rev.* **D86**, 104030 (2012), arXiv:1208.1437 [gr-qc].
- [14] James Lucietti, Keiju Murata, Harvey S. Reall, and Norihiro Tanahashi, “On the horizon instability of an extreme Reissner-Nordström black hole,” *JHEP* **1303**, 035 (2013), arXiv:1212.2557 [gr-qc].
- [15] Keiju Murata, Harvey S. Reall, and Norihiro Tanahashi, “What happens at the horizon(s) of an extreme black hole?” *Class.Quant.Grav.* **30**, 235007 (2013), arXiv:1307.6800.
- [16] Ivan Booth and Stephen Fairhurst, “Isolated, slowly evolving, and dynamical trapping horizons: Geometry and mechanics from surface deformations,” *Phys. Rev.* **D75**, 084019 (2007), arXiv:gr-qc/0610032 [gr-qc].
- [17] S. W. Hawking and G. F. R. Ellis, *The Large Scale Structure of Space-time* (Cambridge University Press, 1973).
- [18] S.A. Hayward, “General laws of black hole dynamics,” *Phys.Rev.* **D49**, 6467–6474 (1994).
- [19] Abhay Ashtekar and Badri Krishnan, “Isolated and dynamical horizons and their applications,” *Living Rev.Rel.* **7**, 10 (2004), arXiv:gr-qc/0407042 [gr-qc].
- [20] Abhay Ashtekar and Gregory J. Galloway, “Some uniqueness results for dynamical horizons,” *Adv.Theor.Math.Phys.* **9**, 1–30 (2005), arXiv:gr-qc/0503109 [gr-qc].
- [21] Raphael Bousso and Netta Engelhardt, “New Area Law in General Relativity,” *Phys. Rev. Lett.* **115**, 081301 (2015), arXiv:1504.07627 [hep-th].
- [22] Ivan Booth, “Black hole boundaries,” *Can.J.Phys.* **83**, 1073–1099 (2005), arXiv:gr-qc/0508107 [gr-qc].
- [23] L. Andersson, M. Mars, and W. Simon, “Local existence of dynamical and trapping horizons,” *Phys.Rev.Lett.* **95**, 111102 (2005), arXiv:gr-qc/0506013 [gr-qc].
- [24] Lars Andersson, Marc Mars, and Walter Simon, “Stability of marginally outer trapped surfaces and existence of marginally outer trapped tubes,” *Adv. Theor. Math. Phys.* **12**, 853–888 (2008), arXiv:0704.2889 [gr-qc].
- [25] Ivan Booth and Stephen Fairhurst, “Extremality conditions for isolated and dynamical horizons,” *Phys.Rev.* **D77**, 084005 (2008), arXiv:0708.2209 [gr-qc].
- [26] Sergio Dain, Jose Luis Jaramillo, and Martin Reiris, “Area-charge inequality for black holes,” *Class.Quant.Grav.* **29**, 035013 (2012), arXiv:1109.5602 [gr-qc].
- [27] Ivan Booth and Stephen Fairhurst, “The first law for slowly evolving horizons,” *Phys.Rev.Lett.* **92**, 011102 (2004), arXiv:gr-qc/0307087 [gr-qc].
- [28] Ivan Booth, Lionel Brits, Jose A. Gonzalez, and Chris Van Den Broeck, “Marginally trapped tubes and dynamical horizons,” *Class. Quant. Grav.* **23**, 413–440 (2006), arXiv:gr-qc/0506119 [gr-qc].
- [29] Tony Chu, Harald P. Pfeiffer, and Michael I. Cohen, “Horizon dynamics of distorted rotating black holes,” *Phys.Rev.* **D83**, 104018 (2011), arXiv:1011.2601 [gr-qc].
- [30] I. Ben-Dov, “The Penrose inequality and apparent horizons,” *Phys.Rev.* **D70**, 124031 (2004), arXiv:gr-qc/0408066 [gr-qc].
- [31] William Kavanagh and Ivan Booth, “Spacetimes containing slowly evolving horizons,” *Phys.Rev.* **D74**, 044027 (2006), arXiv:gr-qc/0603074 [gr-qc].
- [32] W.B. Bonnor and P.C. Vaidya, “Spherically symmetric radiation of charge in Einstein-Maxwell theory,” *Gen.Rel.Grav.* **1**, 127–130 (1970).
- [33] CJS Clarke and Tevian Dray, “Junction conditions for null hypersurfaces,” *Classical and Quantum Gravity* **4**, 265 (1987).
- [34] C. Barrabes and W. Israel, “Thin shells in general relativity and cosmology: The Lightlike limit,” *Phys. Rev.* **D43**, 1129–1142 (1991).
- [35] Marc Mars and Jose M. M. Senovilla, “Geometry of general hypersurfaces in space-time: Junction conditions,” *Class. Quant. Grav.* **10**, 1865–1897 (1993), arXiv:gr-qc/0201054 [gr-qc].
- [36] Eric Poisson, *A Relativist’s Toolkit* (Cambridge University Press, 2004).
- [37] A. Ori, “Charged null fluid and the weak energy condition,” *Class.Quant.Grav.* **8**, 1559 (1991).
- [38] W. Israel, “Singular hypersurfaces and thin shells in general relativity,” *Nuovo Cimento B*, **44**, 1–14 (1966).
- [39] Catherine Williams, “A Black hole with no marginally trapped tube asymptotic to its event horizon,” in *4th International Conference on Complex Analysis and Dynamical Systems Nahariya, Israel, May 18-22, 2009* (2010) arXiv:1005.5401 [gr-qc].
- [40] L. Andersson, M. Mars, J. Metzger, and W. Simon, “The time evolution of marginally trapped surfaces,” *Class.Quant.Grav.* **26**, 085018 (2009), arXiv:0811.4721 [gr-qc].
- [41] Benjamin K. Tippett and Ivan Booth, “Closest Safe Approach to an Accreting Black Hole,” *Phys. Rev.* **D90**, 084027 (2014), arXiv:1406.4039 [gr-qc].